NUMERICAL STUDY OF THE UPPER OCEAN RESPONSE OF THE WESTERN CARIBBEAN SEA TO HURRICANE MITCH

Jinyu Sheng[1*], Liang Wang[2], Bo Yang[1], Serge Andréfouët[3],
Chuanmin Hu[2], Bruce G. Hatcher[4], and Frank E. Muller-Karger[2]

[1]Department of Oceanography, Dalhousie University
Halifax, Nova Scotia, Canada

[2]College of Marine Science, University of South Florida
St. Petersburg, FL 33701, USA

[3]Institut de Recherche pour le Développement
Noumea Cedex, New-Caledonia

[4]Marine Ecosystem Research, Cape Breton University
Sydney, Nova Scotia, Canada

1. INTRODUCTION

The main objective of this study is to examine the circulation and hydrographic distribution in the upper ocean of the western Caribbean Sea during Hurricane Mitch in 1998 using a nested-grid ocean circulation model. Mitch was one of the most disastrous storms in history to strike the central American countries. The storm originated from a tropical wave over western Africa on October 8, 1998 and Mitch moved through the eastern Caribbean Sea on October 18 and 19 (http://www.nhr.noaa.gov). It intensified from a tropical depression to a hurricane in the southwestern Caribbean Sea on October 22 (Figure 1), with a maximum wind speed of ~55 km h^{-1}. The storm strengthened to a category-5 hurricane storm by October 26, with a maximum sustained wind speed of ~285 km h^{-1}. From October 27, Mitch skirted the north coast of Honduras and then became nearly stationary over Guanaja in the Bay Islands for over 24 hours, eventually drifting slowly south. The storm made landfall over Honduras in the morning of October 29, with a maximum wind speed of ~160 km h^{-1}. Mitch progressed inland to the south then westward over the mountainous regions of Honduras and Guatemala. During its passage, Mitch generated significant precipitation over much of Nicaragua, Honduras, and Guatemala, which in turn caused flooding and land slides and massive river discharge to the adjacent coast (Guiney and Lawrence, 1999; Smith et al., 2002).
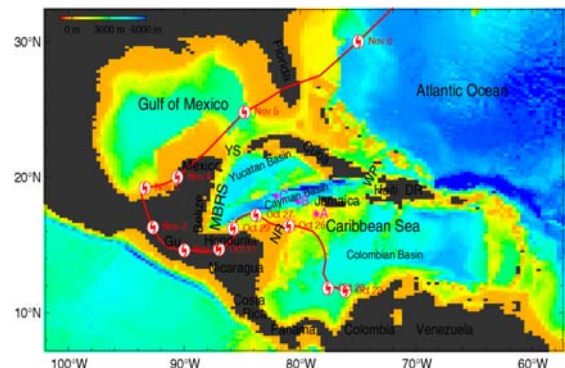

Figure 1. Topographic map of the Gulf of Mexico and Caribbean Sea and the storm track (red line) of Hurricane Mitch from October 22 to November 6, 1998. The storm symbol along the storm track denotes the beginning location of the storm center on each day. Abbreviations are used for the Mesoamerican Barrier Reef System (MBRS), Yucatan Strait (YS), Gulf of Honduras (GOH), Guatemala (Gu), Nicaragua Rise (NR), Dominican Republic (DR) and Windward Passage (WP).

* *Corresponding author address*: Jinyu Sheng, Department of Oceanography, Dalhousie University, Halifax, Nova Scotia, B3H 4J1, Canada, e-mail: Jinyu.Sheng@Dal.Ca

High-resolution (1.1 km/pixel at nadir) ocean color data from the Sea-viewing Wide Field-of-view Sensor (SeaWiFS) were captured and processed using the software package SeaDAS4.4 at the University of South Florida. Images from an earlier processing were used to demonstrate the connection of nearshore and offshore areas of the northwestern Caribbean Sea (Andréfouët et al., 2002). Figure 2 shows the contrast between the distributions of chlorophyll-a concentration before (Figure 2a) and after (Figures 2c and d) Hurricane Mitch. On October 24, when Mitch was still far from the Mesoamerican Barrier Reef System (MBRS), turbid water was restricted to the Honduras coast and Belize shelf. After Mitch, the turbid plume extended from the northeast coast of Honduras to the deep ocean, the Bay Islands (150 km, eastward, Figure 2b), and further north to the Belize shelf on November 3 (Figure 2c).
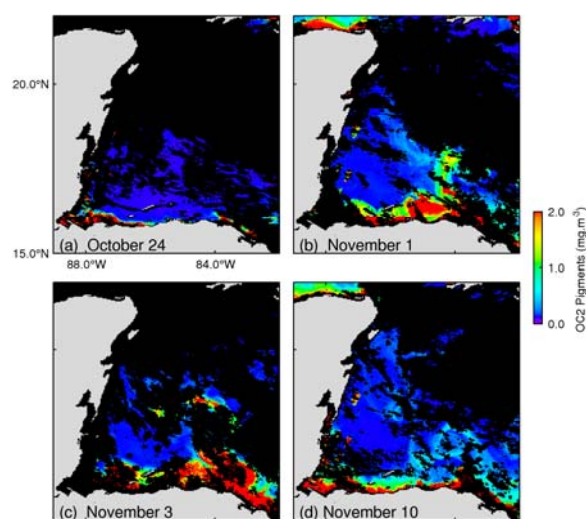

Figure 2: Spatial patterns of turbid coastal water plumes over the northwestern Caribbean Sea derived from SeaWiFS remote sensing data during and after Hurricane Mitch (Andréfouët et al., 2002). Clouds and land are masked as purple and grey colors, respectively. (a) Typical dry season conditions showing clear ocean and narrow zones of turbidity near river mouths. (b) First high-quality image 3 days after landfall of Mitch showing a large-scale plume that covered most of the Bay Islands and extended to 200 km from its origin. (c) The coastal water plume extended further northward to reach Glovers atoll on the Belize shelf. (d) The plume dissipated by dilution.

2. CIRCULATION MODEL AND FORCING

A triply nested-grid ocean circulation modeling system is used in this study. The nested-grid system was constructed from a primitive-equation z-level model known as CANDIE, which stands for the Canadian version of Diecast (Sheng et al., 1998). The nested-grid system has three subcomponents (Figure 3): a coarse resolution outer model (~19 km) covering the western Caribbean Sea (WCS, 72-90°W and 8-24°N), an intermediate resolution middle model (~6 km) covering the Mesoamerican Barrier Reef System (MBRS, 84-89°W, 15.5-20°N), and a fine resolution inner model (~2 km) covering the northern coast of Honduras and the Bay Islands (85-88°W, 15.6-17°N). The nested system uses the digital bathymetric database of 2-minute resolution (DBDB2) developed by the Ocean Dynamics and Prediction Branch, Naval Research Laboratory of the United States. The boundary definitions of the middle and inner model domains are justified here by the geographic location of the MBRS along the Mexico-Belize-Honduras coast, and the significant impact of Hurricane Mitch in 1998 on the Honduras coast, from where most of the coastal runoff plumes detected by the SeaWiFS originated.

The three subcomponents of the nested system have the same 28 unevenly spaced z-levels, with a finest vertical resolution of 2 m in the top ten levels, and relatively coarse vertical resolution of about 500 m at depths of greater than 1000 m.

The nested-grid system uses the sub-grid scale mixing parameterization suggested by Price (1981) for the vertical eddy viscosity and diffusivity coefficients K_m and K_h. The horizontal mixing scheme of Smagorinsky (1963) is used to parameterize the horizontal eddy viscosity and diffusivity coefficients (A_m, A_h), which are related to the model grid spacing, and velocity shear and strain in the horizontal direction. The nested system also uses the fourth-order numerical technique (Dietrich, 1997) and flux limiter to discretize the nonlinear advection terms (Thuburn, 1996).

The two-way nesting technique based on the smoothed semi-prognostic method developed by Sheng et al. (2005) is used to exchange information between three subcomponents of the nested-grid system. A free-slip boundary condition is used at lateral solid boundaries in the three subcomponents of the nested system. Along open boundaries of each subcomponent, the normal flow, temperature and salinity fields are updated using adaptive open boundary conditions. The depth-mean normal flows across the outer model open boundaries are set to be

the monthly mean results produced by a $(1/3)°$ Atlantic model based on FLAME. The outer (middle) model results are used to specify the boundary conditions along the open boundaries of the middle (inner) models.

The nested-grid system is forced by 6 hourly wind stress, monthly mean heat and freshwater fluxes at the sea surface, and climatologically time-mean freshwater discharges from 11 major rivers in the WCS in the first 294 days (i.e., from January 1 to October 21) of 1998. The 6 hourly wind stress is converted from 6 hourly wind velocity extracted from the National Centers for Environmental Prediction (NCEP) of the National Oceanic and Atmospheric Administration (NOAA) and the National Center for Atmospheric Research (NCAR) 40 year reanalysis (Kalnay et al., 1996). The conventional bulk formula of Large and Pond (1981) is used to convert NCEP/NCAR wind velocities to wind stresses.
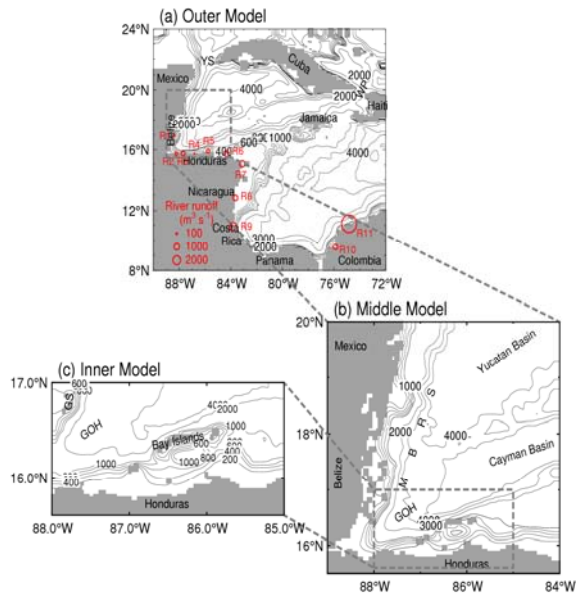

Figure 3: Selected bottom topographic features for the triply nested-grid modeling system consisting of (a) an outer model covering western Caribbean Sea (WCS); (b) a middle model including the southern Mesoamerican Barrier Reef System (MBRS); and an inner model zooming in the north coast of Honduras and Bay Islands. Isobaths are labeled in units of meters, and red open circles denote the mouth positions of 11 major rivers specified in the modeling system. The strength of the time-mean discharge of each river is denoted by the area of each circle.

The net heat flux through the sea surface Q_{net} is expressed according to Barnier et al., (1995):

$$Q_{net} = Q_{net}^{c} + \gamma(SST^{c} + SST^{m}) \qquad (1)$$

where Q_{net}^{c} is the monthly mean net heat flux taken from da Silva et al. (1994), SST^{c} is the monthly mean sea surface temperature climatology, SST^{m} is the model calculated sea surface temperature, and γ is the coupling coefficient defined as $z_1 \rho_o c_p / \tau_Q$, where z_1 is the thickness of the top z-level, c_p is the specific heat, and τ_Q is the restoring time scale which is set to 10 days except for a special area in Campeche near the Yucatan Strait where the restoring time scale is set to 5 days. The model sea surface salinity is also restored to the monthly mean climatology at a time scale of 10 days to approximate the sea surface freshwater fluxes.

Eleven major rivers are specified in the nested-grid system (see Figure 3a for positions of river mouths), with the climatologically time-mean discharge of each river taken from estimates made by Mastin and Olsen (2002), Smith et al. (2002) and a United Nations report (UNCEP/GEF, 2002). All 11 rivers are defined in the top z-level in the nested system and each river is approximated by one grid wide and three grids long in the outer model, one grid wide and five grids long in the middle model, and three grids wide and ten grids long in the inner model. The time-mean discharge of each river is specified in the term of the vertical velocity at the bottom at the head of each river. Based on the conservation of salt, the model salinity (S_r^{n}) at the river head is specified as

$$S_r^{n} = \frac{S_r^{n-1} \cdot V_c + S_0 \cdot V_r}{V_c + V_r} \qquad (2)$$

where S_r^{n-1} is the model salinity at the head of the river at the previous time step; S_0 is the salinity of river waters at the head, which is set to 0.4 psu; V_c is the volume of the model cell at the head of the river; and V_r is the volume of freshwater discharge from the river during one time step. The above specification of the salinity and discharge at the river head allows the buoyant estuarine waters to flow freely into the WCS with the model salinity at the river

head and mouth varying according to the strength of the river discharge.

For the next 20 days of model simulations from October 22 to November 10, the nested-grid system is integrated with three additional forcing associated with the storm. The first additional forcing is a simple vortex to represent the wind stress associated with a moving storm (Chris Fogarty, personal communication, 2006):

$$\tau(r) = \begin{cases} \tau_{max} \dfrac{r}{r_{min}} & r < r_{min} \\ \tau_{max} \dfrac{r_{max} \, r_{min}}{r_{max} - r_{min}} (\dfrac{1}{r} - \dfrac{1}{r_{max}}) & r_{min} \leqslant r \leqslant r_{max} \\ 0 & r > r_{max} \end{cases} \quad (3)$$

where $\tau(r)$ is the cyclonic wind stress as a function of radius r with respect to the center of the moving storm, τ_{max} is the amplitude of the maximum wind stress located at r_{min}, and r_{max} is the outer radius where τ vanishes. Here, r_{min} is set to 20 km and r_{max} to 300 km based on the satellite images during Hurricane Mitch, and τ_{max} to be the maximum wind stress calculated from the observed maximum sustained wind speed provided by the Southeast Regional Climate Center (SERCC). The realistic storm track provided by SERCC is also used (Figure 1), with the instantaneous translational speeds of Hurricane Mitch calculated from the 6-hourly SERCC storm track data.

Figure 4 shows the combination of the NCEP/NCAR wind stress and the simple vortex at day 298.5 (1200 October 26), when the vortex reaches the northern flank of the Nicaragua Rise, with a maximum stress of about 10 N m^{-2}. The vortex approaches the northern coast of Honduras and made landfall in the early morning of October 29, with a maximum stress of ~2.5 N m^{-2}.

The second additional forcing is the buoyancy forcing associated with Mitch-induced precipitation in the open ocean. The daily mean precipitations in the WCS during Mitch interpolated from the 1°x1^{o} global precipitation dataset constructed by Huffman et al. (2001) from multi-satellite observations are used in this study. For the first order of accuracy, we assume that the evaporation during Mitch was small in comparison with the storm-induced precipitation, and estimate the model salinity in the top z-level affected by the Mitch-induced precipitation (S_1^n) based on

$$S_1^n = \frac{\hat{S}_1^n \cdot \Delta z_1}{\Delta z_1 + \Delta z_p} \qquad (4)$$

Where $\hat{S}_1^n$ is the model salinity at the top z-level before the modification; Δz_1 is the thickness of the top z-level; and Δz_p is the thickness of the rainfall during one time step.
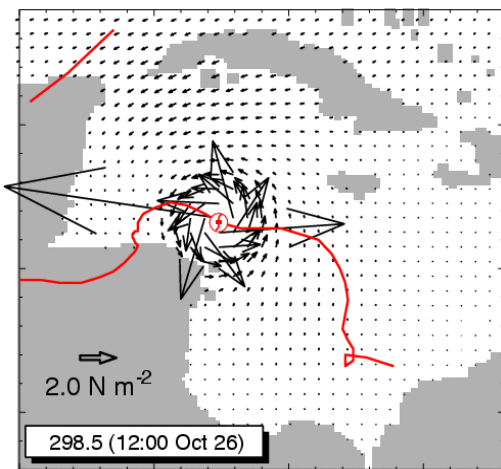

Figure 4: Combined wind stress based on 6 hourly NCEP/NCAR fields and a simple vortex at day 298.5 (12:00 Oct. 26). Wind stress vectors are plotted at every third model grid of the outer model.
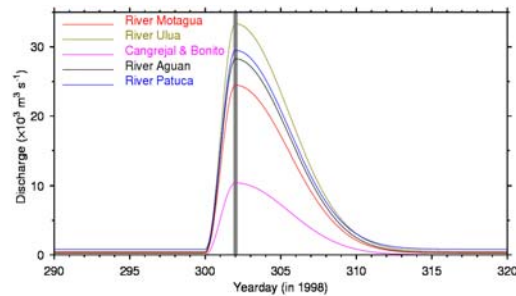

Figure 5: Time series of freshwater discharges from five major rivers in Honduras to the southern Meso-American Barrier Reef System during Hurricane Mitch.

The third additional forcing is the buoyancy forcing associated with storm-induced discharges from 5 major rivers in Honduras and Guatemala (i.e., the Motagua, Ulua, Cangreja, Bonito, and Aguan Rivers) during Mitch. Mitch

generated heavy rainfall and intense river flooding over central and southern Honduras after making landfall and introduced massive freshwater discharges to the southern MBRS (Smith et al., 2002). The peak discharge (estimated from indirect measurements, see Smith et al., 2002) from the five major rivers during Mitch was ~1.3×10^5 m^3 s^{-1}, which is about 70 times more than the climatologically time-mean discharge of ~1.9×10^3 m^3 s^{-1}. Since there were no direct river gauge measurements for the five major rivers during Mitch, time series of the storm-induced runoff from these five rivers are constructed (Figure 5) by assuming the Mitch-induced flood processes of the 5 rivers started at day 300.0, reached the peak discharge at day 302.0 and then decreased exponentially in time with an e-folding time of 5 days.

3. MODEL RESULTS

The nested-grid circulation system is initialized with the monthly mean climatology of temperature and salinity in January constructed from hydrographic observations at the standard z-levels extracted from the World Ocean Database 1998 compiled by the US National Oceanographic Data Center (NODC), using the objective analysis technique known as Barnes' algorithm (Geshlin et al., 1999). The nested-grid system is first integrated for 294 days from January 1 to October 21 in 1998 forced by monthly mean surface heat and freshwater fluxes, 6-hourly NCEP/NCAR wind stress, and climatologically time-mean discharges from 11 major rivers in the WCS. Three additional forcings described above are added to the model forcing for the next 20 days of integration from October 22 to November 10. Figure 6 shows an example of simulated near-surface (1.0 m) currents produced by the nested-grid modeling system.

After Mitch intensified from a tropical depression to a hurricane in the southern Colombian Basin on October 22, the simulated near-surface circulation in the southern Caribbean Sea was most strongly affected, with divergent, near-surface currents of ~1 m s^{-1} forced by the local wind field over an area around the storm center in the southern Colombian Basin, with a radius of influence approximating 100 km on October 23 (day 295.5). Outside this area of influence, the near-surface circulation produced by the outer

model is very similar to the near-surface circulation under normal (no storm) conditions, which is characterized by a relatively broad and approximately westward flow associated with the Caribbean Current in the northern and central Colombian Basin (Ezer et al., 2005; Sheng and Tang, 2003 and 2004; Tang et al., 2006, Oey et al., 2007).

At 1200 UTC October 26 (day 298.5) Mitch reached the northern flank of the Nicaragua Rise as a fully developed, category-5 hurricane. The near-surface currents produced by the outer model in the WCS have been affected significantly by Mitch by this time. There are intense, divergent near-surface currents forced by the local wind under the storm over the Cayman Basin, and strong near-inertial currents in the wake of the storm over the northern Colombian Basin; a result consistent with studies of storm-induced circulations elsewhere (Chang and Anthes, 1978; Price, 1981; Greatbatch, 1983; Sheng et al., 2006). The middle and inner model results at day 298.5 demonstrate that the storm also significantly affected the near-surface circulation on the MBRS, with a broad and approximately westward flow exceeding 0.5 m s^{-1} velocity over the central region of the reef system.
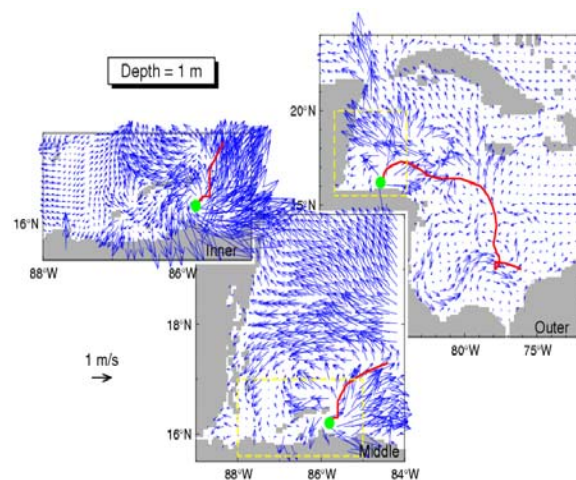

Figure 6: Simulated near-surface currents at day 301.0 (0000 UTC October 29) just before Mitch made landfall on the northern Honduras coast with a sustained wind speed of 205 km h^{-1}. The red line represents the storm track and solid green circle represents the location of the storm center at this time. Velocity vectors are plotted at every third model grid point.

As Hurricane Mitch approached the northern coast of Honduras and made landfall in the early morning of October 29, the nested-grid model results for a few hours before landfall demonstrate that the near-surface circulation in the WCS is significantly affected by Mitch (Figure 6), with intense and divergent near-surface currents of ~4 m s^{-1} over the coastal waters between the Bay Islands and the northern coast of Honduras, strong northwestward currents over the western Yucatan Basins and intense northward through-flow over the western part of the Yucatan Strait. The middle and inner models generate stronger divergent near-surface currents over the southern MBRS than the outer model, as expected. The middle model also produces strong, westward or northwestward near-surface currents of ~2 m s^{-1} over the central MBRS and a strong, southwestward jet over the Belize shelf.

When Mitch moved inland and weakened to a tropical depression on November 1, the near-surface and sub-surface circulations produced by the outer model at day 304.5 (1200 UTC November 1) still have strong, near-inertial currents along the storm track and adjacent areas, particularly over the right side of the track. The nested-grid system generates broad and approximately northwestward currents over the central MBRS, strong eastward coastal currents around the Bay Islands and along the northern coast of Honduras, and stronger-than-usual currents flowing into the Gulf of Mexico through the western part of the Yucatan Strait.

The other important characteristic of the upper ocean response to a hurricane is the generation of a cool wake behind the storm. Previous studies of the storm-induced circulation in a flat bottom ocean (Chang and Anthes, 1978; Price, 1981; Greatbatch, 1983) suggest that the cool water wake is biased to the right of the storm track and strongly dependent on the hurricane translation speed, with greater cooling for a slower moving storm. To elucidate the upper ocean response to Hurricane Mitch, the differences in the near-surface temperature and currents between the model runs with and without the storm are calculated (Figure 7), and referred to as the storm-induced SST cooling and currents. The storm-induced near-surface currents at day 301.5 are horizontally divergent under the storm, with a maximum speed of greater than 5 m s^{-1} (Figure 7a). Behind the storm, there is a cool water pool, which is biased to the right of the storm track. There are strong

near-inertial oscillations and a cool water wake in the vicinity of the storm track, both of which are more intense on the right than on the left of the storm track. As discussed in previous studies (Chang and Anthes, 1978; Price, 1981; Greatbatch, 1983; Sheng et al. 2006), the rightward bias of the near-inertial currents and SST cooling behind the storm can be explained largely by the fact that a more efficient energy transfer from the storm to the ocean occurs on the right side of the storm track than the left side of the storm track in the Northern Hemisphere.

The outer model produces a large area of SST cooling in the southern MBRS at day 301.5, with a maximum thermal loss of about 10°C over the coastal region around the Bay Islands, and weaker SST cooling over the northern flank of the Nicaragua Rise and central Colombian Basin (Figure 7). The storm-induced, near-surface, near-inertial currents are relatively strong and widespread over the northwestern Caribbean Sea, and in the vicinity of the storm track over the central Colombian Basin. Part of the near-inertial energy excited over the northern flank of Nicaragua Rise propagates southward along the east coast of Honduras and reaches the southwestern Colombian Basin at day 301.0. By day 304.5, however, the near-surface cooling and near-inertial currents have largely dissipated and spread to other regions of the WCS.
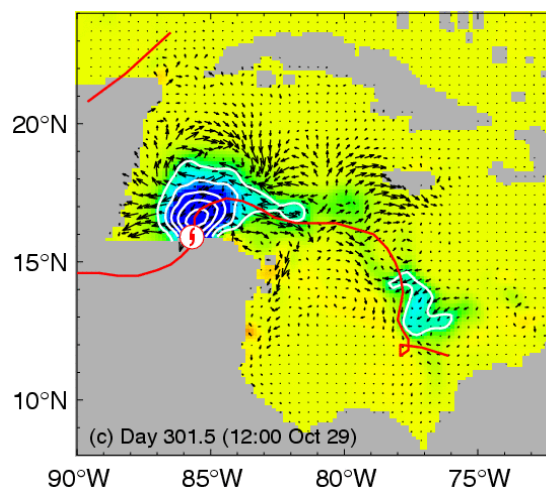

Figure 7: Model-calculated changes in sea surface temperature (SST) and currents associated with Hurricane Mitch at different times produced by the outer model. Contour intervals are 2°C. The red line represents the storm track and the storm symbol represents the location of the storm center. Velocity vectors are plotted at every second grid point.

The performance of the nested-grid system in simulating buoyancy-driven flows resulting from storm-induced freshwater input from five major rivers in Honduras and Guatemala is assessed by comparing the simulated near-surface salinity in the control run with SSS derived from the SeaWiFS ocean color data. The SeaWiFS images depict a large river plume extending from the eastern part of the northern Honduras coast into the deep ocean during Hurricane Mitch (Figure 18a), indicating an important hydrodynamic connection between coral reefs and adjacent coasts after the passage of the storm. Lower salinity waters (<35.5 psu) observed along the northern Honduras coast in the SeaWiFS observations are well captured in the simulated river plumes produced by the middle model in the control run (Figure 8).

At 1200 November 1 (day 304.5) the low-salinity waters are produced by the nested-grid middle model off the northern coast of Honduras with two distinct buoyant estuarine (western and eastern) plumes, which agrees qualitatively with the SeaWiFS images (Figures 8a and b). The western plume, which is produced by the storm-induced discharges from the Ulua, Motagua, Cangrejal, and Bonito Rivers, is located over the GOH, and spreads gradually northeastward with the head of the plume reaching the coastal area of the northwestern Bay Islands by day 304.5. The eastern plume, which is produced by the storm-induced discharges from the Aguan and Patuca Rivers, is located over the coastal region off the eastern part of the northern Honduras coast, and has expanded significantly offshore by day 304.5, with the head of the plume interacting with the westward Caribbean Current over the deep water region to the northeast of the Bay Islands. There is a backward breaking wave along the eastern outer edge of the eastern plume at day 304.5 (Figure 8b), which is a typical feature of baroclinic waves on the density front that have a tendency to break in the upstream direction (Sheng, 2001). At 1200 UTC November 3 (day 306.5), the western plume expands further northeastward to spread over the western and northern coastal regions of the Bay Islands (Figure 8d). The head of the eastern plume at this time turns westward with the Caribbean Current, with a narrow filament connecting the head and the base of the plume near the Honduras coast. Long after Hurricane Mitch's passage the middle model predicts a strong interaction of the two plumes at 1200 UTC

November 14 (day 317.5, Fig. 8f), and the western plume spreads eastward and joins the eastern plume, resulting in continuous occurrence of low-salinity waters along the northern coast of Honduras. The head of the eastern plume has separated from the main body of the plume by this time, and is entrained into an intense cyclonic gyre over the deep water region to the north of the Bay Islands (Figure 8f). Salinity had returned to normal by 7 May, approximately 6 months after the storm passed.
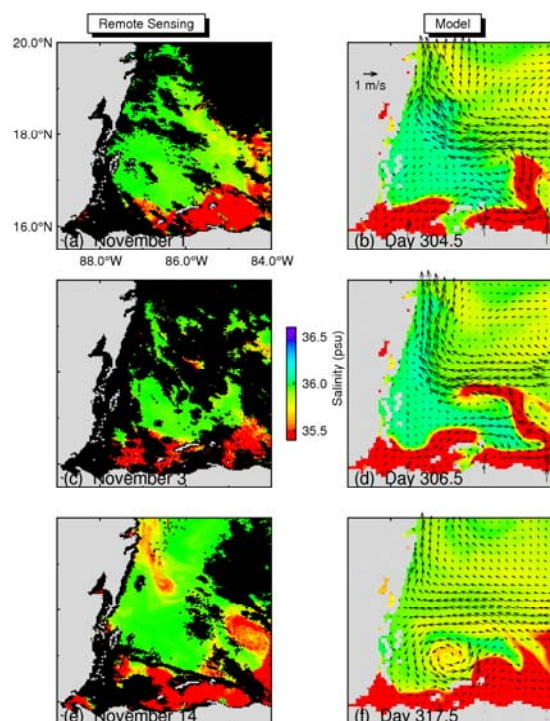

Figure 8: Comparison of spatial patterns of river plumes characterized by the sea surface salinity between the remote sensing data processed through SeaWiFS data (a, c, and e) and the middle model results (b, d, and f) during Hurricane Mitch. Clouds are masked as black color in a, c, and e. Model velocity vectors are plotted at every third grid point.

The model-calculated patterns of spreading plumes defined by low salinity values are visually comparable with those obtained from SeaWiFS observations, with large differences in meso-scale features of the plumes (Figure 8). It is expected that the coarse resolution of the bottom topography (2-minute grid), the idealized parameterizations of the wind forcing associated

with Mitch and the model sub-grid mixing, and the uncertainty of the true flood processes of the major rivers in Guatemala and Honduras could all negatively affect the model performance.

4. SUMMARY

A triply nested-grid ocean circulation modeling system was used to simulate the storm-induced circulation in the western Caribbean Sea and low-salinity coastal water plumes over the southern Meso-American Barrier Reef System in late October 1998 during Hurricane Mitch. The nested-grid system generates strong, divergent surface currents under the storm, and intense near-inertial current oscillations accompanied by cooling of sea surface temperatures behind the storm. Both features are more energetic to the right of the storm track. The system also reproduces well the strong buoyant estuarine

plumes extending from the coast to the deep water region off Honduras, which is consistent with SeaWiFS- derived salinity observations shortly after the passage of Hurricane Mitch.

5. ACKNOWLEDGMENTS

6. REFERENCES

Andréfouët, S., P. J. Mumby, M. McField, C. Hu, and F. E. Muller-Karger, Revisiting coral reef connectivity, *Coral Reefs,* **21**, 43-48, 2002.

Barnier, B., L. Siefridt, and P. Marchesiello, Thermal forcing for a global ocean circulation model using a three-year climatology for ECMWF analyses, *J. Mar. Sys.,* **6**, 363-380, 1995.

Chang, S. W., and R. A. Anthes, Numerical simulations of the ocean's nonlinear baroclinic response to translating hurricanes, *J. Phys. Oceanogr., 8*, 468-480, 1978.

da Silva, A. M., C. C. Young, and S. Levitus, Atlas of surface marine data 1994, Volume 3, Anomalies of heat and momentum fluxes, NOAA Atlas NESDIS 8, 413 pp. NOAA, Washington, DC, 1994.

Dietrich, D. E., Application of a modified Arakawa 'a' grid ocean model having reduced numerical dispersion to the Gulf of Mexico circulation, *Dyn. Atmos. and Oceans,* **27**, 201-217, 1997.

Ezer, T., D. V. Thattai, B. Kjerfve, and W. D. Heyman, On the variability of the flow along the Meso-American Barrier Reef System: a numerical model study of the influence of the Caribbean current and eddies, *Ocean Dyn.*,**55**, 458-475, 2005.

Geshelin, Y., J. Sheng, and R. J. Greatbatch, Monthly mean climatologies of temperature and salinity in the western North Atlantic, *Can. Tech. Rep. Hydrogr. Ocean. Sci*. **153**, 62 pp., 1999.

Greatbatch, R. J., On the response of the ocean to a moving storm: The nonlinear dynamics, schemes, *J. Geophys. Res.,* **13**, 357-367, 1983.

Guiney, J. L., and M. B. Lawrence, Preliminary Report: Hurricane Mitch 22 October-5 November 1998, National Hurricane Centre, Miami, USA, 8 pp., 1999.

Huffman, G. J., R. F. Adler, M. M. Morrissey, D. T. Bolvin, S. Curtis, R. Joyce, B. McGavock, and J. Susskind, Global precipitation at one-degree daily resolution from multisatellite observations, *J. Hydrometeorology*, **2**, 36-50, 2001.

Kalnay, E., and 20 others, The NCEP/NCAR 40-year reanalysis project. *Bull. Am. Meteor. Soc*., **77**, 437-472, 1996.

Large, W. G., and S. Pond, Open ocean momentum flux measurements in moderate to

strong winds, *J. Phys. Oceanogr.,* **11**, 324-336, 1981.

Mastin, M. C., and T. D. Olsen, Fifty-year storm-tide flood-inundation maps for Santa Rosa de Aguan, Honduras, Water-Resources Investigations Report 02-258, U.S. Geological Survey, 2002.

Oey, L-Y, T. Ezer, D.-P. Wang, X.-Q. Yin, and S.-J. Fan, Hurricane-induced motion and interaction with ocean currents, *Cont. Shelf. Res*., doi:10.10.1016/j./csr.2007.01.008, 2007.

Price, J. F., Upper ocean response to a hurricane, *J. Phys. Oceanogr.,* **11**, 153-175, 1981.

Sheng, J., and L. Tang, A numerical study of circulation in the western Caribbean Sea, *J. Phys. Oceanogr.,* **31**, 3146-3163, 2003.

Sheng, J., and L. Tang, A two-way nested-grid ocean-circulation model for the Meso-American Barrier Reef System, *Ocean Dyn.,* **54**, 232-242, 2004.

Sheng, J., R. J. Greatbatch, X. Zhai, and L. Tang, A new two-way nesting technique based on the smoothed semi-prognostic method, *Ocean Dyn.,* **55**, doi:10.101007/sl0236-005-0005-6, 162-177, 2005.

Sheng, J., D. G. Wright. R. J. Greatbatch, and D. E. Dietrich, CANDIE: A new version of the DieCAST ocean circulation model, *J. Atmos. and Ocean. Tech.,* **15**, 1414-1432, 1998.

Sheng, J., X. Zhai, and R. J. Greatbatch, Numerical study of the storm-induced circulation on the Scotian Shelf during Hurricane Juan using a nested-grid ocean model, *Prog. in Oceanogr.*, **70**, doi:10.1016/ j.pocean.2005.07.007, 233-254, 2006.

Smagorinsky, J., General circulation experiments with the primitive equation. I. The basic experiment, *Mon. Wea. Rev*., **21**, 99-165, 1963.

Smith, M. E., J. V. Phillips, and N. E. Spahr, Hurricane Mitch: peak discharge for selected river reaches in Honduras, Water-Resources Investigations Report 01-4266, U.S. Geological Survey, 2002.

Tang, L., J. Sheng, B. G. Hatcher, and P. F. Sale, Numerical study of circulation, dispersion and hydrodynamic connectivity of surface waters on the Belize shelf, *J. Geophys. Res.,* **111**, C01003, doi:10.1029/2005JC002930, 2006.

Thuburn, J., Multidimensional flux-limited advection schemes, *J. Comput. Phys.,* **123**, 74-83, 1996.

UNCEP/GEF, Regionally based assessment of persistent toxic substances in Central America and the Caribbean, Global Environment facility, United Nations Environment Programme Chemicals, Chatelaine, Switzerland, 133 pp., 2002.